Songklanakarin J. Sci. Technol.
44 (2), 401-407, Mar. - Apr. 2022

http://www.sjst.psu.ac.th

Original Article

One-dimensional tight-binding model for electron transport through ferromagnet/insulator/ferromagnet junction in B-field

Natthagrittha Nakhonthong*, and Puangratana Pairor

School of Physics, Institute of Science, Suranaree University of Technology, Mueang, Nakhon Ratchasima, 30000 Thailand

Received: 19 March 2021; Revised: 20 July 2021; Accepted: 21 September 2021

Abstract

We applied a one-dimensional tight-binding model to the study electron transport in a ferromagnetic metal-insulator-ferromagnetic metal junction. We included a small external magnetic field perpendicular to the one-dimensional chain as a Zeeman Effect on electron spins. We obtained the transmission and reflection probabilities of an electron across the junction and used them to calculate its tunneling magnetoresistance. We found that the magnetoresistance ratio increases with the insulating gap of the insulator. The variation of the insulator thickness gives an oscillating behavior of the ratio. Our theoretical model predicts the right trend of the magnetoresistance on the thickness, and also indicates that at a certain thickness the maximum magnetoresistance ratio occurs.

Keywords: tight-binding model, tunneling magnetoresistance, ferromagnet/insulator interface

1. Introduction

Electronic devices, like diodes and transistors, contain junctions acting as barriers for charge carriers in the devices to tunnel through. The flow of these carriers is characterized by the electronic properties of the device materials and can be manipulated by applied external fields. In 1988, the Grünberg's and Fert's research groups showed that we can control the particle transport through junctions with magnetic field as well. In that year both groups independently discovered giant magnetoresistance in thin film multilayered structures of alternating ferromagenetic metals separated by a metallic non-magnetic spacer (Baibich *et al.*, 1988; Binasch, Grünberg, Saurenbach, & Zinn, 1989). That is, they found that the resistances of their samples can be significantly changed by applied magnetic field. In the absence of the field, the resistance of the system is high, because the magnetizations of two adjacent ferromagnetic layers are in opposite direction. When the field is turned on and strong enough, the magnetizations become in parallel resulting in much lower resistance. This effect allows us to control the current flow, by making use of the spin degree of freedom. This discovery marked the birth of the field of spintronics that studies the manipulation and control of spin degree of freedom in electronic devices by means of electric and magnetic field. From the point of view of practical application, giant magnetoresistance has since attracted interest from makers of magnetic sensors, switches, logical devices, read heads for hard disc drives, and random-access memory devices, and spin-field effect transistors (Awschalom, Epstein, & Hanson, 2007; Chappert, Fert, & Van Dau, 2010; Julie Grollier *et al.*, 2001; Katine, Albert, Buhrman, Myers, & Ralph, 2000).

Many experimental research works have shown that there are several factors impacting on the change in resistance with the field, or the magnetoresistance ratio. For instance, to be able to observe the giant magnetoresistance, the thickness of the metallic non-magnetic layer between two adjacent ferromagnetic layers has to be in the order of nanometers (S. Parkin, More, & Roche, 1990), because at these distances only does the Ruderman-Kittel-Kasuya-Yosida (RKKY) interaction between the two ferromagnetic layers cause their magnetizations to be antiparallel in zero magnetic fields (Kasuya, 1956; Ruderman & Kittel, 1954; Yosida, 1957). Grünberg and co-workers were among the first to observe this antiferromagnetic interlayer interaction between two ferromagnetic layers decaying regularly with increasing non-

*Corresponding author
Email address: nakhonthong@gmail.com

magnetic spacer thickness (Grünberg, Schreiber, Pang, Brodsky, & Sowers, 1986). Once the magnetizations of two ferromagnetic layers are antiparallel in zero field, a strong enough field can force them to be in parallel. The reduction of resistance with the field usually hits a plateau at some value of field strength H_S, which depends on the thickness of the spacer and the number of spacer layers (Fert & Campbell, 1968; J Grollier *et al.*, 2003; Mosca *et al.*, 1991). Also, if one replaces the metallic non-magnetic spacer with an insulating layer, the percentage of the magnetoresistance ratio (called tunneling magnetoresistance ratio) is more pronounced (Butler, Zhang, Schulthess, & MacLaren, 2001; Coll *et al.*, 2019; Fang, Zang, Xiao, Zhong, & Tao, 2020; LeClair *et al.*, 2002; Mathon & Umerski, 2001; S. S. Parkin *et al.*, 2004; Scheike *et al.*, 2021; Yuasa, Nagahama, Fukushima, Suzuki, & Ando, 2004).

Theoretically, we can understand the experimental results through quantum mechanics. In 1975, Julliére used the result from transfer Hamiltonian method, sometimes called Bardeen's approach, to explain his experimental results. He measured the conductance of the junction of two different ferromagnetic electrodes separated by insulating layer in applied magnetic field. In the absence of the field, the magnetizations of both electrodes were in parallel, because the thickness of the insulating layer was too big for the RKKY interaction to cause them to be antiparallel. However, once the field was turned on and its strength was between the two coercive fields of the two ferromagnets, the magnetizations would be in opposite directions and he observed the reduction of 14% in the conductance (Julliere, 1975). He quantitatively explained the experimental results, using the transfer Hamiltonian method. In this approach, high insulating barrier potential (or low tunneling regime) and elastic tunneling are assumed. As a result, the conductance is proportional to product of the densities of states for majority spin and minority spin of the two ferromagnetic electrodes (Bardeen, 1961). In Julliére's case, the magnetic field causes the shift in the densities of states and hence the reduction of the conductance. Due to the low tunneling regime assumption valid in Julliére's case, the quantitative results from this approach are limited to cases of insulating barriers, whereas other aspects, like the effects of non-insulating barriers and barrier thickness, cannot be explored.

To examine such effect of the thickness insulating layer and also that of relative direction of the magnetizations of the two electrodes in the absence of applied field, Slonczewski (Slonczewski, 1989) modeled the same type of junction using a one-electron model. He solved the Schrodinger equation for the system to obtain the transmission probability in the elastic scattering process. He found that the thickness and the potential barrier would affect the conductance. Also, the conductance would depend on the angles between the two magnetizations. The Slonczewski model works well with the junction consisting of the metallic ferromagnets with electronic parabolic energy dispersion. It was shown by Qi and coworkers (Qi, Xing, & Dong, 1998) that Slonczewski's model can be applied to a wider range of cases than Julliere's model, and it gives the same results as Julliere's model, when the barrier potential is very high (Qi *et al.*, 1998).

When the effect of realistic energy band structure of either ferromagnetic layers or the spacer on this type of junction is of interest, researchers turn to First-principles calculation. Once they obtain the realistic band structures, they use the Green's function technique to calculate the conductance. For instance, Waldron, Timoshevskii, Hu, Xia, and Guo (2006) studied the transport of electrons through clean Fe (100)/MgO (100)/Fe (100) structure (Waldron *et al.*, 2006) and found that the zero-bias tunnel magnetoresistance of this junction could be many thousand percent. However, the effect can be reduced when the Fe/MgO interface is oxidized. Results are limited to the case of low tunneling regime and in zero applied magnetic field.

Another method of calculation used to study this type of junction in the literature is a tight-binding model. It is used to obtain a non-parabolic energy dispersion relation of electrons in the system. It is not as realistic as the first-principles calculation, but similar to that in Slonczewski's model, it allows us to include arbitrary barrier potential into the calculation of transmission probability. However, like in Slonczewski's model, for most studies of the magnetic tunneling junction with a tight-biding model the direct inclusion of the effect of the magnetic field has not much been investigated. In our work, we include a small applied magnetic field into a one-dimensional tight-binding model to investigate how the electronic properties and the thickness of the insulating layer affect the flow of electrons across a ferromagnet/insulator/ferromagnet junction.

2. Materials and Methods

We model our system as an infinite chain of a ferromagnet/ insulator/ ferromagnet junction as depicted in Figure 1. We label each site by an index n and $|n\sigma\rangle$ is the electron orbital state at site n with spin σ. There are two ferromagnetic metal regions, to the left and to the right of the insulating layer. That is, the insulating ions are on the sites with $0 \le n \le N_I$. In our calculation we assume the following: electrons in the system are not interacting with one another, the particle transport through the system is ballistic, only one atomic orbital contributes to the electron eigenstate of the system, only nearest- neighbor hopping energy is significant, the lattice constant of the system is the same in all regions (we take into account the possible unequal lattice constants by adjusting the hopping energy, where it is needed) , the magnetizations of the two ferromagnetic metals are in opposite directions at zero magnetic field, and the applied field is small enough for us to consider it as a Zeeman Effect. The Hamiltonian of system is written as

$$\hat{H} = \hat{H}_L + \hat{H}_I + \hat{H}_R \tag{1}$$

where $\hat{H}_L, \hat{H}_I, \hat{H}_R$ describe the ferromagnetic metal on the left, the insulating layer, and the ferromagnetic metal on the right respectively. Each term is written as follows.

$$\begin{aligned}\hat{H}_L = (\varepsilon_L - \mu_L) & \sum_{n=-\infty}^{-1} \sum_{\sigma=\downarrow}^{\uparrow} |n\sigma\rangle\langle n\sigma| \\ & - t_L \sum_{n=-\infty}^{-2} \sum_{\sigma=\downarrow}^{\uparrow} (|n\sigma\rangle\langle n+1,\sigma| + c.c.) \\ & - (J_L \\ & + cB) \sum_{n=-\infty}^{-1} (|n\uparrow\rangle\langle n\uparrow| \\ & - |n\downarrow\rangle\langle n\downarrow|)\end{aligned}$$

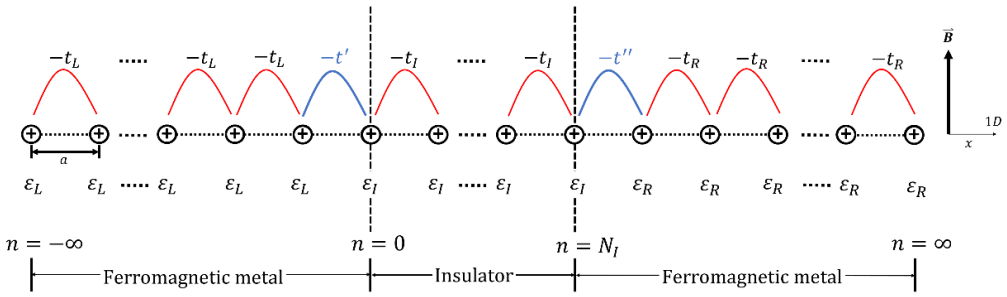

Figure 1. Chain of ions that represents one-dimensional the ferromagnetic metal/insulator/ferromagnetic metal junction

$$\hat{H}_I = -t' \sum_{\sigma=\downarrow}^{\uparrow} (|-1\sigma\rangle\langle 0\sigma| + c.c.) + (\varepsilon_I - \mu_I) \sum_{n=1}^{N_I} \sum_{\sigma=\downarrow}^{\uparrow} |n\sigma\rangle\langle n\sigma| - t_I \sum_{n=1}^{N_I-1} \sum_{\sigma=\downarrow}^{\uparrow} (|n\sigma\rangle\langle n+1,\sigma| + c.c.) - t'' \sum_{\sigma=\downarrow}^{\uparrow} (|N_I\sigma\rangle\langle N_I+1,\sigma| + c.c.) - \sum_{n=1}^{N_I} cB(|n\uparrow\rangle\langle n\uparrow| - |n\downarrow\rangle\langle n\downarrow|)$$

$$\hat{H}_R = (\varepsilon_R - \mu_R) \sum_{n=N_I+1}^{\infty} \sum_{\sigma=\downarrow}^{\uparrow} |n\sigma\rangle\langle n\sigma| - t_R \sum_{n=N_I+1}^{\infty} \sum_{\sigma=\downarrow}^{\uparrow} (|n\sigma\rangle\langle n+1,\sigma| + c.c.) - (-J_R + cB) \sum_{n=N_I+1}^{\infty} (|n\uparrow\rangle\langle n\uparrow| - |n\downarrow\rangle\langle n\downarrow|).$$

Here, ε_i, μ_i are the on-site energies and the chemical potentials for region i respectively, t's are the corresponding nearest neighbor hopping energies (t' and t'' are the hopping energies at the two interfaces), and J_L,J_R are the magnitudes of the spin exchange energies of the two ferromagnetic metals. Also, B is the magnetic field and c is an appropriate proportional constant.

The energy dispersion relation for an electron with spin σ in the bulk of each material is thus as follows:

$$E_{k\sigma,L} = (\varepsilon_L - \mu_L) - 2t_L \cos(k_{L\sigma}a) \mp J_L \mp cB \quad (5)$$

$$E_{k\sigma,I} = (\varepsilon_I - \mu_I) - 2t_I \cos(k_{I\sigma}a) \mp cB \quad (6)$$

$$E_{k\sigma,R} = (\varepsilon_R - \mu_R) - 2t_R \cos(k_{R\sigma}a) \pm J_R \mp cB. \quad (7)$$

The upper and lower sign are for $\sigma = \uparrow$ and $\downarrow$ respectively. In the ballistic limit and the approximation that the electron energy does not change, while it moves within the system; that is, $E_{k\sigma,L} = E_{k\sigma,I} = E_{k\sigma,R} = E$.

The electron wave function in each region can be written as a summation the corresponding one-electron states:

$$|\phi_{\sigma L}\rangle = \sum_{n=-\infty}^{-1} c_{n\sigma,L}|n\sigma\rangle \quad (8)$$

$$|\phi_{\sigma I}\rangle = \sum_{n=0}^{N_I} c_{n\sigma,I}|n\sigma\rangle \quad (9)$$

$$|\phi_{\sigma R}\rangle = \sum_{n=N_I+1}^{\infty} c_{n\sigma,R}|n\sigma\rangle \quad (10)$$

where $c_{n\sigma,L}$, $c_{n\sigma,R}$ and $c_{n\sigma,I}$ are the amplitudes of one-electron state with spin σ at site n in the three corresponding regions.

A schematic diagram of electron states for a scattering event, in which an incident electron injected from the left side of the system, is shown in Figure 2. There are two possibilities for the incident event: one with the incident electron with spin $\uparrow$ and the other with spin $\downarrow$. The amplitudes of $|\phi_{\sigma L}\rangle$ are then

$$\begin{bmatrix} c_{n\uparrow,L} \\ c_{n\downarrow,L} \end{bmatrix} = \begin{bmatrix} 1 \\ 0 \end{bmatrix} e^{ik_{L\uparrow}na} + r_\uparrow \begin{bmatrix} 1 \\ 0 \end{bmatrix} e^{-ik_{L\uparrow}na} + r_\downarrow \begin{bmatrix} 0 \\ 1 \end{bmatrix} e^{-ik_{L\downarrow}na}, \quad (11)$$

for the case, where the incident electron has with spin $\uparrow$, and when the incident electron with spin $\downarrow$, the amplitudes are

$$\begin{bmatrix} c_{n\uparrow,L} \\ c_{n\downarrow,L} \end{bmatrix} = \begin{bmatrix} 0 \\ 1 \end{bmatrix} e^{ik_{L\downarrow}na} + r_\uparrow \begin{bmatrix} 1 \\ 0 \end{bmatrix} e^{-ik_{L\uparrow}na} + r_\downarrow \begin{bmatrix} 0 \\ 1 \end{bmatrix} e^{-ik_{L\downarrow}na}. \quad (12)$$

r_σ are the reflection coefficients of the reflected electron waves with spin σ. The wave vector of a spin electrons is $k_{L\sigma}$, and $k_{L\sigma} = \frac{1}{a}\cos^{-1}\left(\frac{(\varepsilon_L-\mu) \mp J_L \mp cB-E}{2t_L}\right)$, where now μ is the chemical potential of the system and the upper and lower signs are for state with $\sigma = \uparrow$ and $\downarrow$ respectively.

We can now write the amplitudes of $|\phi_{\sigma I}\rangle$ as,

$$\begin{bmatrix} c_{n\uparrow,I} \\ c_{n\downarrow,I} \end{bmatrix} = \begin{bmatrix} \alpha_\uparrow \\ 0 \end{bmatrix} e^{ik_{I\uparrow}na} + \begin{bmatrix} 0 \\ \alpha_\downarrow \end{bmatrix} e^{ik_{I\downarrow}na} + \begin{bmatrix} \beta_\uparrow \\ 0 \end{bmatrix} e^{-ik_{I\uparrow}na} + \begin{bmatrix} 0 \\ \beta_\downarrow \end{bmatrix} e^{-ik_{I\downarrow}na} \quad (13)$$

where α_σ and β_σ are the amplitudes of electrons with spin σ in the insulating region. $k_{I\sigma} = \frac{1}{a}\cos^{-1}\left(\frac{(\varepsilon_I-\mu) \mp cB-E}{2t_I}\right)$, where the upper and lower signs are for state with $\sigma = \uparrow$ and $\downarrow$ respectively. We now write $\varepsilon_I - \mu = \frac{\Delta}{2} + 2t_I$ where Δ is the insulating energy gap.

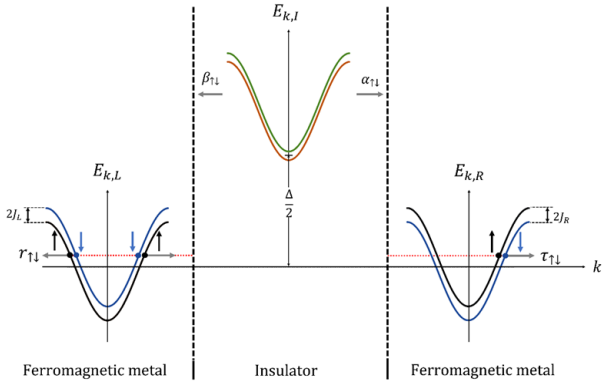

Figure 2. Sketches of the electron energy dispersion relation in each region in the presence of applied magnetic field

Amplitudes of $|\phi_{\sigma R}\rangle$ then are

$$\begin{bmatrix} c_{n\uparrow,R} \\ c_{n\downarrow,R} \end{bmatrix} = \tau_{\uparrow} \begin{bmatrix} 1 \\ 0 \end{bmatrix} e^{ik_{R\uparrow}na} + \tau_{\downarrow} \begin{bmatrix} 1 \\ 0 \end{bmatrix} e^{ik_{R\downarrow}na}. \quad (14)$$

τ_σ are the transmission amplitudes of the outgoing electron waves with spin σ. $k_{R\sigma} = \frac{1}{a}\cos^{-1}\left(\frac{(\varepsilon_R - \mu) \pm J_R \mp cB - E}{2t_R}\right)$, where the upper and lower sign are again for state with $\sigma =\uparrow$ and $\downarrow$ respectively.

We obtain all the reflection and transmission amplitudes by solving the following matching conditions, which are from considering the system Hamiltonian and the ballistic condition:

$$t_L c_{0\sigma,L} = t' c_{0\sigma,I} \quad (15)$$

$$t_I c_{-1\sigma,I} = t' c_{-1\sigma,L} \quad (16)$$

$$t_L c_{N_I\sigma,I} = t'' c_{N_I\sigma,R} \quad (17)$$

$$t_I c_{(N_I+1)\sigma,I} = t'' c_{(N_I+1)\sigma,R}\,. \quad (18)$$

The transmission and reflection probabilities are spin-dependent and are described in the equations below. In the case of the incident electron with spin ↑, there are two different reflection probabilities and two transmission probabilities:

$$R_{\uparrow}^{incident\uparrow} = |r_{\uparrow}|^2 \quad (19)$$

$$R_{\downarrow}^{incident\uparrow} = |r_{\downarrow}|^2 \frac{\sin(k_{L\downarrow}a)}{\sin(k_{L\uparrow}a)} \quad (20)$$

$$T_{\uparrow}^{incident\uparrow} = |\tau_{\uparrow}|^2 \frac{t_R}{t_L}\frac{\sin(k_{R\uparrow}a)}{\sin(k_{L\uparrow}a)} \quad (21)$$

$$T_{\downarrow}^{incident\uparrow} = |\tau_{\downarrow}|^2 \frac{t_R}{t_L}\frac{\sin(k_{R\downarrow}a)}{\sin(k_{L\uparrow}a)}. \quad (22)$$

Similarly, In the case of the incident electron with spin ↓, there are two different reflection probabilities and two transmission probabilities:

$$R_{\uparrow}^{incident\downarrow} = |r_{\uparrow}|^2 \frac{\sin(k_{L\uparrow}a)}{\sin(k_{L\downarrow}a)} \quad (23)$$

$$R_{\downarrow}^{incident\downarrow} = |r_{\downarrow}|^2 \quad (24)$$

$$T_{\uparrow}^{incident\downarrow} = |\tau_{\uparrow}|^2 \frac{t_R}{t_L}\frac{\sin(k_{R\uparrow}a)}{\sin(k_{L\downarrow}a)} \quad (25)$$

$$T_{\downarrow}^{incident\downarrow} = |\tau_{\downarrow}|^2 \frac{t_R}{t_L}\frac{\sin(k_{R\downarrow}a)}{\sin(k_{L\downarrow}a)}. \quad (26)$$

We write the net current density of spin-σ electron across a junction, with an applied voltage V in an applied field B across the junction of thickness d and with electric field $\mathbb{E}$, as

$$j_{net}^{\sigma} = \sum_k ev_\sigma T_\sigma(k,B)[f(\varepsilon_{k\sigma} - eV) - f(\varepsilon_{k\sigma})] \quad (27)$$

where e is the magnitude of an electron charge, $T_\sigma(k,B)$ is the transmission probability of a spin σ electron, $f(\varepsilon)$ is the Fermi-Dirac distribution function, and v_σ is the velocity of the spin σ electron. Changing the summation in to an integral, we have for one dimensional system,

$$j_{net}^{\sigma} = \frac{Le}{2\pi}\int dk v_\sigma T_\sigma(k,B)[f(\varepsilon_{k\sigma} - eV) - f(\varepsilon_{k\sigma})] \quad (28)$$

Because $v_\sigma = \frac{1}{\hbar}\frac{d\varepsilon_{k\sigma}}{dk}$,

$$j_{net}^{\sigma} = \frac{Le}{2\pi\hbar}\int_{-\infty}^{\infty} d\varepsilon_{k\sigma} T_\sigma(\varepsilon_{k\sigma},B)\,[f(\varepsilon_{k\sigma} - eV) - f(\varepsilon_{k\sigma})]. \quad (29)$$

At low enough temperature,

$$j_{net}^{\sigma} = \frac{Le}{h}\int_{\mu}^{\mu+eV} d\varepsilon_{k\sigma} T_\sigma(\varepsilon_{k\sigma},B) \quad (30)$$

$$j_{net}^{\sigma} = \frac{Le^2}{h} T_\sigma(\mu,B)V. \quad (31)$$

Therefore, the conductivity κ of the junction for a junction of thickness d is

$$\kappa_\sigma(\mu,B) = \frac{Le^2 d}{h} T_\sigma(\mu,B). \quad (32)$$

Once we obtain $T_\sigma(\mu,B)$ for each case, we can examine closely how physical properties of the insulating layer affects the magnetoresistance ratio (MR) of our junction.

We will ultimately calculate MR from the conductivity. That is,

$$\text{MR} = \frac{\sum_\sigma \kappa_\sigma(\mu,B) - \sum_\sigma \kappa_\sigma(\mu,0)}{\sum_\sigma \kappa_\sigma(\mu,0)} \quad (33)$$

where the second term of the numerator is referred to the conductance of the junction when both ferromagnetic electrodes have opposite magnetizations and the first term of the numerator is the conductance as a function of the applied field (Julliere, 1975). When $cB \geq 2J_R$, both ferromagnetic electrodes have parallel magnetizations.

3. Results and Discussion

For all our results, we assign our parameters of both ferromagnetic metals with the values related to the known physical properties of Fe. Also, all the energy terms in our model are taken to be with respect to the hopping energy of conduction electrons in Fe. Here is the list of the physical

quantities of Fe we use in our work: 1) the exchange energy is approximately $2J = 0.089$ eV, approximated from the Curie temperature of Fe, 2) the hopping energy of Fe is taken to be about $t = 0.93$ eV, approximated from the Fe d-band width (Walter, Riley, & Rader, 2010; Yamasaki & Fujiwara, 2002), and 3) the proportional constant c related to the applied field is taken to be the magnetic dipole moment of Fe, equal to $2.22\mu_B = 0.13$ meV/T, where μ_B is the Bohr magneton. From these values, we set $t_L = t_R = t$ and $J_L = J_R = 0.05t$. Also, in order to model the middle layer to be an insulator, we set the related parameters accordingly. That is, $\varepsilon_I - \mu = \frac{\Delta}{2} + 2t_I$ must be in such a way that $\Delta > 0$.

In Figure 3 we present the results of our model to be compared with the experimental result of Fe/MgO/Fe junction from Yuasa and coworkers. The experimental result in Figure 3(a) shows an oscillating behavior over a period of about two atomic layers of MgO, which is unchanged with temperature (Yuasa *et al.*, 2004). Our theoretical model can provide the result as shown in Figure 3(b), depicting the oscillations of similar periods. The model suggests that the MR period of oscillations may depend on the strength of an applied field. Nevertheless, there are a few important experimental features, for which our model cannot account. As can be seen in Figure 3(b), our theoretical MR shows the increasing trend in both baseline value and its oscillation amplitude, as the number of MgO layers increases. However, in Figure 3(a) the experiment shows that baseline of MR saturates at around eight layers of MgO and the amplitudes shows a decrease with the number of MgO layers. These shortcomings are due to the fact that our model is for purely one-dimensional system, which in turn would work well only with systems with smooth junctions. If there exists some roughness at interfaces, the MR would saturate and the amplitude of oscillation should decrease with the thickness of the spacer as suggested in the work by Autes and coworkers (Autès, Mathon, & Umerski, 2011).

In Figure 4(a), we show the plots of MR as a function of the applied field for several thicknesses of the insulating layer. The hopping energy at the two interfaces are taken to be the same $t' = t'' = 0.8t$ and we set $\varepsilon_I - \mu = 2.01t$. In our model, MR also shows oscillating behavior with the magnetic field, where its period of oscillation decreases with the increase of the thickness of the insulating layer. Interestingly, the "critical" value of applied magnetic field (B_c), at which MR is maximum, is smaller for thicker insulating layer. Our result also suggests that as long as the condition of antiparallel magnetizations for the two ferromagnetic metals at zero field stills meet (Faure-Vincent *et al.*, 2002; Fert & Campbell, 1968; J Grollier *et al.*, 2003; Mosca *et al.*, 1991), thicker layer can give us a higher MR. However, if we keep the applied field fixed, there is an optimal number of insulating atomic layer for that field to reach a higher value of MR as suggested by the plots in Figure 5.

Our model also allows us to explore the effect of the quality of the interfaces on MR by adjusting the hopping parameters t' and t'', the two hopping energies between the two atoms at the two interfaces. As seen in Figure 6(a), which is the case where $t' = t''$ and we set $N_I = 7$ atoms, when both are smaller than the value of t in the bulk of the ferromagnetic metals, MR is bigger and the corresponding B_c is also smaller. For $t' \neq t''$, both MR and B_c are dictated by the smaller hopping energy.

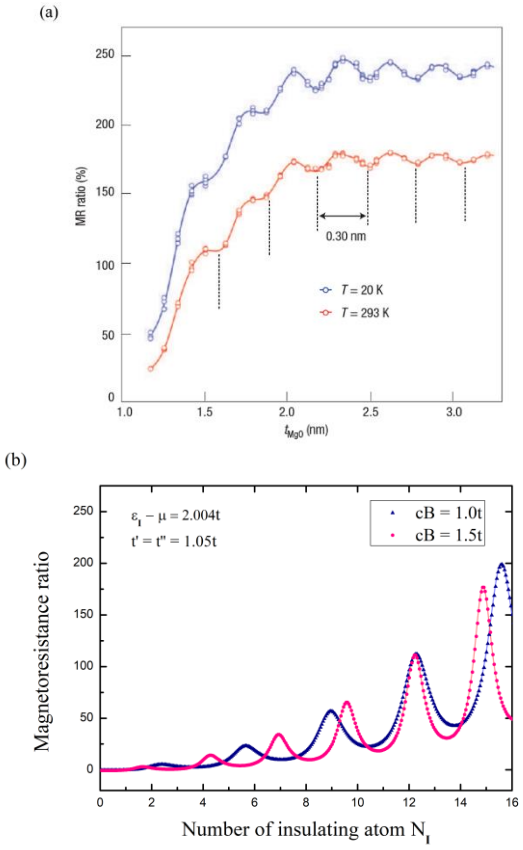

Figure 3. (a) Experimental result of magnetoresistance of Fe/MgO/Fe junction vs thicknesses of MgO from Yuasa *et al.* (2005). (b) Plot of magnetoresistance vs the number of insulating atoms from our model

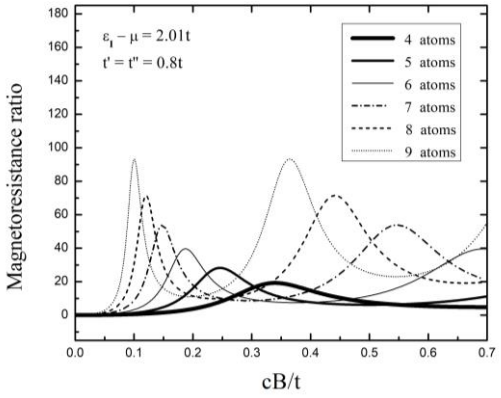

Figure 4. Magnetoresistance ratio as a function of applied magnetic field for various thicknesses of the insulating layer: $N_I = 4$ - 9 atomic layers

The last aspect we explore using our model is how the energy gap of the insulating layer affect MR. In Figure 7, we show MR vs the energy gap for three thicknesses of the insulating layers at $cB = 0.1t$. Our model predicts that for each thickness there is an optimal value of energy gap that can achieve a maximum MR. This suggests that the energy gap of the insulating layer sets the limit of value of MR.

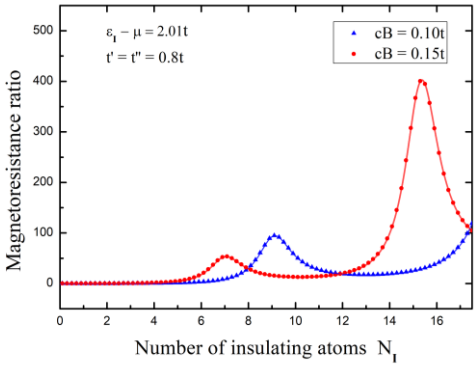

Figure 5. Magnetoresistance ratio as a function of thickness of the insulating layer for two values of applied magnetic field: $cB = 0.1t$ and $0.15t$

4. Conclusions

In this work, we investigate the effect of the insulating layer on the magnetoresistance of a Fe/ insulator/ Fe junction using a one- dimensional tight binding model. Expectedly, the magnetoresistance ratio shows oscillation behavior depends on the strength of the applied magnetic field and the thickness of the thickness of the insulating layer. Our model suggests that to achieve high value of the magnetoresistance ratio, one should do the following: 1) One should make the Fe/ insulator/ Fe junction with the insulator as thick as possible, as long as that thickness allows the two Fe's to have antiparallel magnetizations in zero applied field. 2) At the two interfaces the hopping energy should be lower than that in the bulk of Fe. 3) There is an optimal value of the insulating energy gap that limits the maximum value of the magnetoresistance ratio.

Acknowledgements

This work was financially supported by Research Center for Theoretical Physics of Suranaree University of Technology.

References

Autès, G., Mathon, J., & Umerski, A. (2011). Oscillatory behavior of tunnel magnetoresistance in a magnetic tunnel junction with varying magnetic layer thickness. *Physical Review B, 84*(13), 134404.

Awschalom, D. D., Epstein, R., & Hanson, R. (2007). The diamond age of spintronics. *Scientific American, 297*(4), 84-91.

Baibich, M. N., Broto, J. M., Fert, A., Van Dau, F. N., Petroff, F., Etienne, P., . . . Chazelas, J. (1988). Giant magnetoresistance of (001) Fe/(001) Cr magnetic superlattices. *Physical Review Letters, 61*(21), 2472.

Bardeen, J. (1961). Transfer Hamiltonian of solid tunneling structure. *Physical Review Letters, 6*, 57.

Binasch, G., Grünberg, P., Saurenbach, F., & Zinn, W. (1989). Enhanced magnetoresistance in layered magnetic structures with antiferromagnetic interlayer exchange. *Physical Review B, 39*(7), 4828.

Butler, W., Zhang, X.-G., Schulthess, T., & MacLaren, J. (2001). Spin-dependent tunneling conductance of Fe| MgO| Fe sandwiches. *Physical Review B, 63*(5), 054416.

Chappert, C., Fert, A., & Van Dau, F. N. (2010). The emergence of spin electronics in data storage. *Nanoscience and Technology: A Collection of Reviews from Nature Journals*, 147-157.

Coll, M., Fontcuberta, J., Althammer, M., Bibes, M., Boschker, H., Calleja, A., . . . Dkhil, B. (2019). Towards oxide electronics: A roadmap. *Applied Surface Science, 482*, 1-93.

Fang, H., Zang, X., Xiao, M., Zhong, Y., & Tao, Z. (2020). Oscillations of tunneling magnetoresistance on bias voltage in magnetic tunnel junctions with periodic grating barrier. *Journal of Applied Physics, 127*(16), 163902.

Faure-Vincent, J., Tiusan, C., Bellouard, C., Popova, E., Hehn, M., Montaigne, F., & Schuhl, A. (2002). Interlayer magnetic coupling interactions of two ferromagnetic layers by spin polarized tunneling. *Physical Review Letters, 89*(10), 107206.

Fert, A., & Campbell, I. (1968). Two-current conduction in nickel. *Physical Review Letters, 21*(16), 1190.

Grollier, J., Cros, V., Hamzic, A., George, J.-M., Jaffrès, H., Fert, A., . . . Legall, H. (2001). Spin-polarized current induced switching in Co/Cu/Co pillars. *Applied Physics Letters, 78*(23), 3663-3665.

Grollier, J., Cros, V., Jaffres, H., Hamzic, A., George, J., Faini, G., . . . Fert, A. (2003). Field dependence of magnetization reversal by spin transfer. *Physical Review B, 67*(17), 174402.

Grünberg, P., Schreiber, R., Pang, Y., Brodsky, M., & Sowers, H. (1986). Layered magnetic structures: Evidence for antiferromagnetic coupling of Fe layers across Cr interlayers. *Physical Review Letters, 57*(19), 2442.

Julliere, M. (1975). Tunneling between ferromagnetic films. *Physics Letters A, 54*(3), 225-226.

Kasuya, T. (1956). A theory of metallic ferro-and antiferromagnetism on Zener's model. *Progress of Theoretical Physics, 16*(1), 45-57.

Katine, J., Albert, F., Buhrman, R., Myers, E., & Ralph, D. (2000). Current-driven magnetization reversal and spin-wave excitations in Co/Cu/Co pillars. *Physical Review Letters, 84*(14), 3149.

LeClair, P., Ha, J., Swagten, H., Kohlhepp, J., Van de Vin, C., & De Jonge, W. (2002). Large magnetoresistance using hybrid spin filter devices. *Applied Physics Letters, 80*(4), 625-627.

Mathon, J., & Umerski, A. (2001). Theory of tunneling magnetoresistance of an epitaxial Fe/MgO/Fe (001) junction. *Physical Review B, 63*(22), 220403.

Mosca, D., Petroff, F., Fert, A., Schroeder, P., Pratt Jr, W., & Laloee, R. (1991). Oscillatory interlayer coupling and giant magnetoresistance in Co/Cu multilayers. *Journal of Magnetism and Magnetic Materials, 94*(1-2), L1-L5.

Parkin, S., More, N., & Roche, K. (1990). Oscillations in exchange coupling and magnetoresistance in metallic superlattice structures: Co/Ru, Co/Cr, and Fe/Cr. *Physical Review Letters, 64*(19), 2304.

Parkin, S. S., Kaiser, C., Panchula, A., Rice, P. M., Hughes, B., Samant, M., & Yang, S.-H. (2004). Giant tunnelling magnetoresistance at room temperature with MgO (100) tunnel barriers. *Nature Materials, 3*(12), 862-867.

Qi, Y., Xing, D., & Dong, J. (1998). Relation between Julliere and Slonczewski models of tunneling magneto resistance. *Physical Review B, 58*(5), 2783.

Ruderman, M. A., & Kittel, C. (1954). Indirect exchange coupling of nuclear magnetic moments by conduction electrons. *Physical Review, 96*(1), 99.

Scheike, T., Xiang, Q., Wen, Z., Sukegawa, H., Ohkubo, T., Hono, K., & Mitani, S. (2021). Exceeding 400*%* tunnel magnetoresistance at room temperature in epitaxial Fe/MgO/Fe (001) spin-valve-type magnetic tunnel junctions. *Applied Physics Letters, 118*(4), 042411.

Slonczewski, J. C. (1989). Conductance and exchange coupling of two ferromagnets separated by a tunneling barrier. *Physical Review B, 39*(10), 6995.

Waldron, D., Timoshevskii, V., Hu, Y., Xia, K., & Guo, H. (2006). First principles modeling of tunnel magnetoresistance of Fe/MgO/Fe trilayers. *Physical Review Letters, 97*(22), 226802.

Walter, A. L., Riley, J. D., & Rader, O. (2010). Theoretical limitations to the determination of bandwidth and electron mass renormalization*:* The case of ferromagnetic iron. *New Journal of Physics, 12*(1), 013007.

Yamasaki, A., & Fujiwara, T. (2002). Electronic structure of the M O oxides (M= Mg, Ca, Ti, V) in the GW approximation. *Physical Review B, 66*(24), 245108.

Yosida, K. (1957). Magnetic properties of Cu-Mn alloys. *Physical Review, 106*(5), 893.

Yuasa, S., Nagahama, T., Fukushima, A., Suzuki, Y., & Ando, K. (2004). Giant room-temperature magneto resistance in single-crystal Fe/MgO/Fe magnetic tunnel junctions. *Nature Materials, 3*(12), 868-871.